

Localized Charge Transfer in CsAu·NH₃: ¹H and ¹³³Cs Nuclear Magnetic Resonance

Steffen Krämer and Michael Mehring*

2. Physikalisches Institut, Universität Stuttgart, D-70550 Stuttgart, Germany

Anja-Verena Mudring† and Martin Jansen

Max-Planck-Institut für Festkörperforschung, Heisenbergstrasse 1, D-70569 Stuttgart, Germany

Received: December 3, 2002

We report results from ¹H and ¹³³Cs nuclear magnetic resonance (NMR) studies on CsAu·NH₃. This compound has recently been synthesized and belongs to the family of ammoniates. The intense blue color of the material, which is not observed in the parent compounds, suggests that a charge-transfer electronic state is formed. The ¹H NMR line shape and relaxation rates are found to be very similar to the corresponding properties in pure ammonia. However, the ¹³³Cs-NMR properties of CsAu·NH₃ strongly deviate from the corresponding ones in CsAu, and we show that the former can be interpreted consistently within a localized charge distribution due to either an anharmonic charge density wave state induced by a charge transfer process or an Anderson localization mechanism.

Introduction

Gold exhibits a number of exceptional features with respect to both chemical and physical aspects. They originate from relativistic effects governing the properties of the atomic wave function and energy levels, which are preserved in the metallic state.^{1–3} In particular, the s-orbitals of this material are stabilized by a relativistic radial contraction of the wave function. This enables the formation of an electronic state very close to a metal anion, Au[−], by charge transfer in combination with the most electropositive bonding partners, the alkaline metals.

In the binary compound CsAu, a state is formed that has been described as an ionic alloy or a *charge-transfer insulator*.⁴ The solid phase of this material shows semiconductor-like behavior and has an optical band gap of 2.6 eV.⁵ NMR experiments on CsAu have shown evidence for a melting-induced electron localization from a solid semiconductor to an ionic liquid.⁶

Therefore it is interesting to study the influence of polar solvents such as liquid ammonia on this material. During our investigations of the reaction of CsAu with ammonia, we found that CsAu dissolves readily in liquid ammonia forming a yellow solution. By slowly removing the solvent, however, an interesting effect occurs. CsAu was not recovered directly, but instead, an intense blue solid crystallized, which has been confirmed by structural analysis to be an ammoniate compound of stoichiometry CsAu·NH₃.⁷ Because the color of the compound and the ultraviolet, visual, and near-infrared spectra⁸ resemble blue solutions of alkali metals dissolved in ammonia and because it is well-known that gold(I) readily transfers electron density toward suitable acceptors,⁹ the question about the electronic structure of this new compound arises. Furthermore a charge transfer of electrons into the ammonia system is in particular interesting because it is well-known from experimental and theoretical studies of metal–ammonia solutions that a variety

of physical phenomena occur.^{10,11} The electrons of alkali metals dissolve in ammonia and states of solvated electrons are formed. At low carrier concentration, an isolated state occurs. By increasing the charge concentrations, a bipolaronic state is formed. The high-density state, however, is a liquid metallic state with high conductivity.¹¹ It is therefore very essential to know whether there is some additional evidence for a charge-transfer state in CsAu·NH₃ and how this state can be described by its macroscopic and microscopic properties as charge-transfer concentration or properties of the *solvated electrons*. In particular, it is interesting to know whether the charge-transfer-induced electronic states can be described within a localized or extended state model.

Mössbauer spectroscopy has indicated a reduced 6s-electron density at the Au nucleus as compared with solvent-free CsAu.¹² Magnetic susceptibility measurements, as well as electron paramagnetic resonance spectroscopy (EPR), show no signs of unpaired electrons. Instructive information regarding the electronic structure of CsAu·NH₃, however, has been gained from ¹H- and ¹³³Cs-NMR spectroscopy. NMR investigations were performed in the past on the parent compounds of CsAu·NH₃, namely, CsAu^{4,6,13} and NH₃,¹⁴ with various solutions of alkali metals in ammonia^{15,16} and other materials with localized charge inhomogeneities.¹⁷ They provided important information about structural and dynamical properties of these materials.

General and Structural Properties of CsAu·NH₃

The structure of CsAu·NH₃,⁷ as shown in Figure 1, can be derived from the cubic structure of CsAu by cutting slices of half the face diagonal of the cubic unit cell, remaining parallel to (110). These slabs are separated by a layer of ammonia coordinated to cesium. Ammonia forms nearly rectangular bridges between two Cs atoms as shown on the left side of Figure 1. Its lone pair is directed toward one of the Cs atoms, and consequently, the hydrogen bonding between neighboring ammonia molecules is suppressed because of orientational mismatch. By comparison of the structure of pure cubic CsAu with CsAu·

* To whom correspondence should be addressed. Tel.: +49 (0)711 685 5218. Fax: +49 (0)711 685 5285. E-mail: mehring@physik.uni-stuttgart.de.

† Present address: Ames Laboratory, Iowa State University, 347 Spedding Hall, Ames, Iowa, 50011.

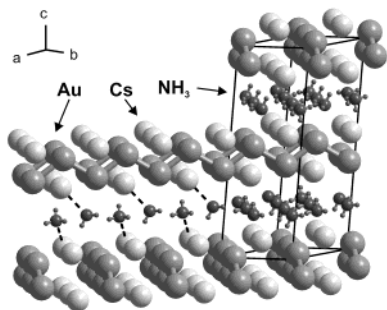


Figure 1. Structure of CsAu·NH₃. On the right side, the unit cell of CsAu·NH₃ is shown together with the intercalated ammonia. On the left side, the ammonia configuration is marked by dashed lines. The ammonia are oriented with their electron pairs toward the Cs atom.

NH₃, it is apparent that a lattice distortion occurs around the Au site in CsAu·NH₃. The Au atoms are shifted toward each other forming zigzag chains with reduced interatomic gold distances. The Au–Au distance is reduced from 426 pm in the pure CsAu compound to 302 pm in CsAu·NH₃.

CsAu·NH₃ is extremely sensitive toward even traces of water and oxidizing agents, such as atmospheric oxygen. The compound decomposes at 225 ± 5 K by separating into CsAu and liquid NH₃. In consequence, all manipulations had to be carried out well below the temperature of decomposition, either under dry argon, in a vacuum, or under ammonia atmosphere. Ammonia (Bayer AG, Leverkusen, Germany) was dried by distilling it first from sodium and then from potassium, where it was stored as a potassium–ammonia solution at 195 K before usage. CsAu was synthesized directly from the elements at 493 K by using an excess of alkali metal, which is distilled off in dynamic vacuum after the reaction has finished. Elementary Cs was prepared by a reduction reaction of CsCl by Ca¹⁸ and further purified by double distillation in a dynamic vacuum. Elementary Au was precipitated by reducing tetrachloric gold acid with sodium oxalate.¹⁹ For the NMR spectroscopic investigations, the ammoniate was synthesized directly in the NMR silica sample containers by condensing liquid ammonia on CsAu, allowing both components to react, and afterward distilling off the excess ammonia. Eventually the sample containers were evacuated and sealed. During this procedure, the samples were cooled in liquid nitrogen to prevent decomposition.

Experimental Details

The NMR measurements were performed on a home-built NMR pulse spectrometer with a variable-temperature insert (VTI) at magnetic fields of 2.3 T for ¹H (100 MHz, tetramethylsilan (TMS)) and 9 T for ¹³³Cs (50 MHz, CsNO₃). We measured spectral line shapes, as well as spin–lattice relaxation rates, for both nuclei in a temperature range from 200 K down to 5 K. The spectra were taken by Fourier transform of the free induction decay after pulse excitation. In the case of ¹³³Cs, we also measured echo spectra by Fourier transform of the second half of the spin–echo. The spin–lattice relaxation rate was determined by applying a saturation recovery sequence. The lineshifts are measured in reference to TMS in the case of ¹H-NMR and a 1-M solution of Cs(NO₃)₃ in the case of ¹³³Cs-NMR.

The CsAu·NH₃ sample was always transferred from a liquid nitrogen Dewar flask into the precooled VTI to prevent decomposition. For comparison, we measured additionally ¹H spectra and spin–lattice relaxation in NH₃, as well as ¹³³Cs in pure CsAu.

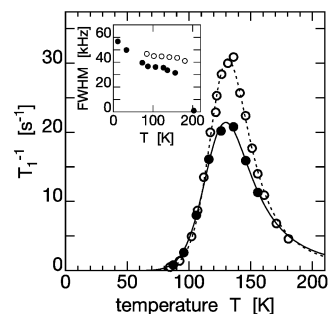


Figure 2. Temperature dependence of ¹H NMR spin–lattice relaxation rate (T_1^{-1}) of CsAu·NH₃ (●) and NH₃ (○). The solid and dotted lines are fits using a modified BPP model of hindered rotations of the ammonia molecule as described in the text. The inset shows temperature dependence of ¹H NMR line width of CsAu·NH₃ (●) and NH₃ (○) expressed as full width at half-maximum (FWHM).

¹H NMR Results and Discussion

The ¹H NMR spectra of CsAu·NH₃ show below 180 K a single resonance line with a weakly temperature-dependent line position. By comparing the line position of NH₃ with CsAu·NH₃, we find in the latter a small but measurable almost temperature-independent diamagnetic shift contribution of about 50 ppm. The observed large shift value is probably due to the diamagnetic susceptibility of the sample.

The ¹H NMR spectral line widths of both compounds increase slightly with decreasing temperature down to 80 K, as shown in the insert of Figure 2. The ¹H line width of the CsAu·NH₃ displays a small change of slope at 110 K with a plateau centered at 100 K and sizable increase below 80 K. In the case of NH₃, the line width behavior was previously analyzed in terms of a dominant H–H dipolar and some smaller contributions of H–N dipolar couplings. The line width is partly reduced at higher temperatures by a rotation of the ammonia molecules around their symmetry axis.¹⁴ The absolute value of the line width in CsAu·NH₃ is about 20% less than that in solid NH₃, which might be explained by a reduced dipolar interaction among the ammonia molecules due to a larger intermolecular distance of the ammonia molecules in CsAu·NH₃ than in NH₃. In the latter, the H–H distance lies between 1.65 Å (neutron diffraction) and 1.82 Å (X-ray).¹⁴ This result implies that the ammonia molecules in CsAu·NH₃ are more dilute than those in solid NH₃ and have the possibility to rotate. The steeper decrease of the ¹H line width with increasing temperature in CsAu·NH₃ compared with that in pure NH₃ suggests that there exists a different motional narrowing mechanism for the ammonia molecules in CsAu·NH₃.

Above 180 K, a sizable narrowing of the ¹H resonance line in CsAu·NH₃ occurs within a narrow temperature range of 10 K. At 185 K, the spectrum shows a superposition of a narrow line with a line width of about 1 kHz and a broad line with 25 kHz line width. Both are centered at –50 ppm/TMS. At 200 K, we recover a single resonance line of 1 kHz line width centered at –40 ppm. We attribute this line narrowing to a melting transition in the NH₃ subsystem leading to rapid diffusion. This temperature is very close to the melting temperature of pure ammonia.

The ¹H NMR spin–lattice relaxation in CsAu·NH₃ shows a strongly temperature-dependent nonexponential relaxation curve with a relaxation maximum at about 130 K. This behavior is well-known in systems with three identical spin ¹/₂ as in molecules containing CH₃ groups, CF₃ groups, or NH₃.^{14,20,21} and has been discussed by applying a model of hindered rotations.^{22,23} For comparison, we measured spin–lattice relax-

TABLE 1: ^1H Spin–Lattice Relaxation Parameters of $\text{CsAu}\cdot\text{NH}_3$, NH_3 (This Work), and NH_3^{14} Obtained by Applying a Model with a Single Mode of Molecular Motion

	$\text{CsAu}\cdot\text{NH}_3$	NH_3 (this work)	NH_3^{14}
E_a [meV]	88 ± 3	106 ± 2	100 ± 1
τ_c^0 [10^{-13} s]	3.7 ± 2	0.83 ± 0.2	1.32 ± 0.4
$\langle\Delta\omega_D^2\rangle$ [$10^9(2\pi\text{ s}^{-1})^2$]	9.4 ± 0.2	13.6 ± 0.2	

ation rates in pure NH_3 with the identical experimental setup and found that the data could be fitted reasonably well by a single-exponential recovery function. We will return to this difference between the two compounds after the quantitative analysis of our results. If we take the initial slope of the spin–lattice relaxation curve of $\text{CsAu}\cdot\text{NH}_3$, we find a temperature dependence very similar to the corresponding spin–lattice relaxation in pure NH_3 as measured by us and in a previous study on NH_3 .¹⁴ The results are shown in Figure 2. If we assume that a single mode of molecular motion governs the spin–lattice relaxation rate, T_1^{-1} is given by a formula proposed by Kubo and Tomita,²⁴ which corrects the classical expression of Bloembergen, Purcell, and Pound (BPP) for this case.²⁵

$$\frac{1}{T_1} = \langle\Delta\omega_D^2\rangle \left(\frac{\tau_c}{1 + (\omega_0\tau_c)^2} + \frac{4\tau_c}{1 + (2\omega_0\tau_c)^2} \right) \quad (1)$$

$\langle\Delta\omega_D^2\rangle$ is of the order of the second moment of the intramolecular proton–proton dipolar interaction, ω_0 denotes the nuclear ^1H Larmor frequency, and τ_c is the correlation time of the molecular motion process. If the motion is thermally activated, the correlation time is given by an Arrhenius equation:

$$\tau_c = \tau_c^0 \exp\left(\frac{E_a}{k_b T}\right) \quad (2)$$

where E_a is the activation energy for the motion and τ_c^0 denotes the correlation time in the infinite temperature limit. In our case, the most likely relaxation path is a rotation of the NH_3 molecule about its symmetry axis, which was previously observed in solid NH_3 .¹⁴ Because there is sizable space between the CsAu blocks of this material, this motion is not expected to be hindered in the $\text{CsAu}\cdot\text{NH}_3$ compound.

We fitted the temperature dependence of the experimental ^1H spin–lattice relaxation rates for $\text{CsAu}\cdot\text{NH}_3$ and pure NH_3 using eqs 1 and 2. The results are shown in Figure 2, together with the experimental data. The corresponding parameters are listed in Table 1. For comparison, we also added spin–lattice relaxation parameters of previously published work.¹⁴

Within this particular relaxation model, our analysis shows that the relevant relaxation parameters are quite similar in $\text{CsAu}\cdot\text{NH}_3$ and pure NH_3 . We find in $\text{CsAu}\cdot\text{NH}_3$ an activation energy, E_a , for the relaxation process that lies about 10% below the activation energy found in pure NH_3 . τ_c^0 is found to be longer in $\text{CsAu}\cdot\text{NH}_3$ compared with pure NH_3 . Finally, the second moment of the relevant interaction $\langle\Delta\omega_D^2\rangle$ is about 30% lower in $\text{CsAu}\cdot\text{NH}_3$ than in NH_3 . This result is consistent with the difference found in the line widths as shown in the insert of Figure 2 and can also be explained by an enlarged intermolecular distance between the ammonia molecules and thus reduced activation energy and interaction strength. Our results clearly show that the ammonia concentration between the CsAu chain layers is reduced compared with solid NH_3 and that the ^1H nuclear spin system becomes more dilute. In conclusion, the observed temperature dependence of the spin–lattice relaxation is governed by the same mechanism in both compounds, $\text{CsAu}\cdot$

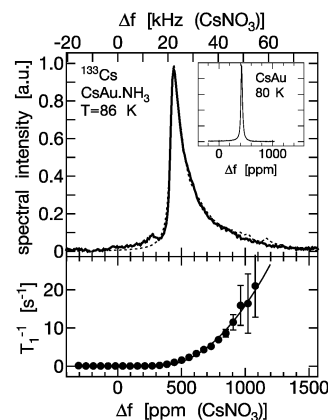


Figure 3. ^{133}Cs -NMR spectrum (top panel) of $\text{CsAu}\cdot\text{NH}_3$ at 86 K (solid line). The data were taken by Fourier transform of the second half of the spin–echo. The dotted line is a fit to the model described in the text. The inset shows the ^{133}Cs -NMR spectra of CsAu at 80 K recorded under the same experimental conditions and displayed using an identical frequency span as for $\text{CsAu}\cdot\text{NH}_3$. The bottom panel shows the frequency shift dependence of spin–lattice relaxation rate (T_1^{-1}) of ^{133}Cs in $\text{CsAu}\cdot\text{NH}_3$ at 86 K (●). The solid line is a fit to a quadratic relation between additional shift contribution and relaxation rate as described in the text.

NH_3 and NH_3 . Because the mechanism in the latter is attributed to a hindered rotation of ammonia around its symmetry axis, this motion is also present in $\text{CsAu}\cdot\text{NH}_3$.

We will now return to the functional form of the spin–lattice relaxation recovery curve. As already mentioned above, the relaxation curve in $\text{CsAu}\cdot\text{NH}_3$ displays a nonexponential behavior, which is not present in pure NH_3 . It is well-known^{26,27} that dilute inhomogeneous spin systems show a nonexponential relaxation behavior due to spin-diffusion processes and a nonhomogeneous spin-temperature distribution. It is very likely that these processes are more relevant in the dilute ammonia layers in the $\text{CsAu}\cdot\text{NH}_3$ compound than in pure NH_3 . This may be related to sizable intrinsic inhomogeneities, which follow from the analysis of the ^{133}Cs results of $\text{CsAu}\cdot\text{NH}_3$ to be shown in the following section.

^{133}Cs NMR Results and Discussion

The ^{133}Cs spectrum of $\text{CsAu}\cdot\text{NH}_3$ shown in Figure 3 for 86 K displays a strongly broadened and asymmetrical line shape, which has not been observed in pure CsAu (cf. insert of Figure 3). The latter shows a narrow almost symmetric resonance line with only a weak temperature dependence between 80 and 350 K. The frequency of the maximum spectral intensity in $\text{CsAu}\cdot\text{NH}_3$ coincides with the spectral line position of CsAu . The latter shows in the temperature range between 80 and 340 K a temperature-independent shift of about 420 ppm, which has been attributed to chemical shift.⁴

^{133}Cs is a spin- $7/2$ nucleus with a gyromagnetic ratio of 5.58 MHz T^{-1} and a nuclear quadrupole moment of $-0.003 \times 10^{-24}\text{ |e| cm}^2$. Powder spectra of quadrupolar nuclei in a noncubic environment are well known to show broad spectra that can be modeled by first- and second-order perturbation theory of the nuclear quadrupole Hamiltonian.²⁸ Because the Cs environment in $\text{CsAu}\cdot\text{NH}_3$ is no longer cubic as in pure CsAu , quadrupole effects might become visible in the Cs spectra. However, it is very unlikely that the observed spectra of $\text{CsAu}\cdot\text{NH}_3$ could be due to first-order quadrupolar effects because this would result in *symmetric* spectra showing a characteristic spin- $7/2$ powder pattern,²⁹ which cannot explain the observed asymmetry. Furthermore, we rule out the possibility of only observing the

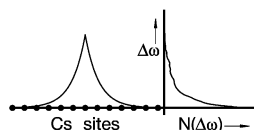


Figure 4. Localized inhomogeneity model for CsAu sites in CsAu·NH₃: (left) additional frequency shift contribution around a particular inhomogeneity site as given by eq 3; (right) resulting frequency histogram, $N(\Delta\omega)$. Further details are given in the text.

central $\pm 1/2$ transition broadened by second-order quadrupolar effects because the Rabi frequency does not change in comparison to liquid Cs(NO₃).²⁹ The $\pi/2$ pulse width that we used was 5 μ s, which is sufficiently strong to excite the whole spectral range. This means that the central and all satellite transitions of the ¹³³Cs nucleus are excited in a nonselective way. In addition, we performed a $\pi/2-\beta$ experiment.³⁰ We found an echo maximum for $\beta = \pi$, which gives further support that the quadrupolar interactions in this compound are weak compared to magnetic interactions.

Another origin of the observed ¹³³Cs-NMR line shape could be due to chemical shift anisotropy (CSA). Because of its large ionic radius, Cs is known to have an easily polarizable electron shell.³¹ In a nonsymmetric environment as in CsAu·NH₃, Cs should therefore display sizable chemical shift anisotropies. In other compounds, Cs-shift anisotropies were reported to be as large as the observed spectral line width in CsAu·NH₃.³² In contrast to the observed spectrum of CsAu·NH₃ however, ¹³³Cs CSA powder spectra show beneath a characteristic maximum intensity at a particular spectral position at least one shoulder, which is not observed here. To rule out any missing edge of a CSA powder spectrum due to frequency-dependent spin–spin relaxation or insufficient excitation bandwidth, we varied the pulse spacing and the excitation frequency.

However, we found no edge or any sign of an asymmetry parameter. Furthermore it would be very unlikely if the spectral position of a CSA-induced singularity coincided with the spectral position of the parent material CsAu as noticed above. In addition, we will show below that a CSA broadening is not consistent with the observed frequency dependence of the spin–lattice relaxation rate. Therefore, we conclude that CSA broadening is not the dominating interaction that causes the observed line shape.

We can also rule out that the observed ¹³³Cs-NMR line shape in CsAu·NH₃ is due to hyperfine interactions of unpaired electrons (*Knight shift*) because there is no paramagnetism observed either in susceptibility or in EPR measurements. Knight shifts of ¹³³Cs are typically on the order 15 000 ppm, whereas our additional shift in CsAu·NH₃ does not exceed 800 ppm.

Because quadrupole, CSA, and hyperfine interactions cannot account for the specific ¹³³Cs line shape in CsAu·NH₃ another explanation is required. Because of results of Mössbauer studies,¹² there is some evidence of reduced electron density at the Au site accompanied by a charge transfer toward the cesium/ammonia system. If the electronic state of the induced carriers becomes localized in the cesium/ammonia system, this would polarize Cs sites next to the inhomogeneity and subsequently induce an additional frequency shift of the ¹³³Cs Larmor frequency. This would result in an inhomogeneous local environment of the Cs site in CsAu·NH₃. A pictorial representation of this scenario is presented in Figure 4. Let us assume that a localized charge near the Cs chain sites introduces a chemical shift, $\Delta\omega$, of the nearby ¹³³Cs nuclei, which depends on the distance r of the nuclei from the localized charge. In Figure 4, we assume an exponential distance dependence of the

chemical shift contributions, $\Delta\omega(r)$, given by

$$\Delta\omega(r) = \Delta\omega_0 \exp\left(-\frac{r}{\xi}\right) \quad (3)$$

where $\Delta\omega_0$ gives the distortion strength and ξ denotes the distortion range. This results in a distribution function $N(\Delta\omega)$ of frequency shifts also presented in Figure 4. By assuming some distribution of local charges with concentration c and adding up all lineshift contributions for a particular Cs site, we have obtained line shapes for the ¹³³Cs NMR line. A random distribution of localized charges fits the observed spectrum displayed in Figure 3. This fit was obtained by using an evolutionary algorithm and provided a concentration c of 2–5% and a distortion range ξ of five lattice parameters. Both parameters, as well as the spectral line position, were found to be weakly temperature-dependent between 80 and 180 K. A commensurate charge density wave would result in a cutoff of the line shape at some frequency and can therefore be excluded.¹⁷ However, we cannot rule out at the moment a nonharmonic charge density wave, which might result in a similar line shape.

Further support for a localized inhomogeneity model is provided by ¹³³Cs spin–lattice relaxation measurements. If we analyze the spin–lattice relaxation of the integrated spectral intensity of the complete ¹³³Cs resonance line, we find a strong nonexponential relaxation behavior. Therefore we extracted the relaxation rate within small spectral windows of the line separately. The spectral width of the window was 3 kHz. Within each spectral window, we find a monoexponential spin–lattice relaxation behavior. The results are shown in Figure 4 at their corresponding spectral positions.

We find an increasing spin–lattice relaxation rate with increasing shift. This provides further support that CSA is not the dominating line broadening mechanism because for CSA powder patterns the frequency dependence of the relaxation rate should follow the opposite behavior as observed here.²⁷ We therefore conclude that the spin–lattice relaxation is governed by inhomogeneously distributed relaxation centers. Because there is a strong correlation between line shift and relaxation rate, these centers are identified with the local charge inhomogeneities responsible for the Cs line shape as discussed in the previous paragraph.

To model shift-dependent relaxation, we assume along the lines of standard NMR relaxation theory that the relaxation rate is proportional to the square of the fluctuating shift, $\Delta\omega^2$, and the corresponding spectral density, $J(\omega_0)$. Combining this with a frequency-independent relaxation rate, $T_{1,b}^{-1}$, leads to the expression

$$\frac{1}{T_1}(\Delta\omega) = \frac{1}{T_{1,b}} + \Delta\omega^2 J(\omega_0) \quad (4)$$

This expression reproduces our experimental data reasonably well, as is presented in Figure 3 (bottom). We find $T_{1,b}^{-1}$ similar to the relaxation rate observed in pure CsAu. We find that $J(\omega_0)$ increases monotonically with temperature between 80 and 170 K with a maximum value of 6×10^{-9} s at 170 K.

Our ¹³³Cs-NMR results strongly suggest an inhomogeneous charge distribution in CsAu·NH₃. So far we can only speculate about its origin. Because a partial charge transfer from the Au site toward the cesium/ammonia regions has been rationalized in ref 7, the following different scenarios might be considered: The transferred charge is dissolved in the ammonia background either as a polaron (charge e , spin $S = 1/2$) or as a bipolaron

(charge $2e$, spin $S = 0$). We can exclude the polaronic state because the sample is EPR silent. A bipolaron, randomly distributed, could well explain the Cs-NMR line shape and relaxation. We note that the observed effects are induced by a charge transfer, which refers to only a few percent of an electron per Au.

The partial charge transfer would lead to a partially filled band structure and correspondingly to a metallic state of the CsAu chains. Because of the one-dimensional nature of these chains, they are susceptible to a periodic lattice distortion and a corresponding charge density wave. If the charge density wave is sufficiently nonharmonic, it might well lead to a similar line shift and relaxation behavior as is reported here.

An alternative explanation of the observed NMR properties could be due to an Anderson localization mechanism,³³ which has been observed in doped semiconductors, as well as metal ammonia solutions.³⁴ It is also based on a partially filled band structure, but the carriers become localized in random potential. The localized state is described by an exponential wave function centered at the localization point r_0 and a localization radius ξ as used in our model for the ^{133}Cs -NMR line shape.

Conclusion

We have measured temperature-dependent ^1H - and ^{133}Cs -NMR line shapes and spin–lattice relaxation rates of the recently synthesized $\text{CsAu}\cdot\text{NH}_3$.

The ^1H NMR data of line position, line width, and spin–lattice relaxation suggest that the dynamic properties of solid ammonia are essentially preserved in $\text{CsAu}\cdot\text{NH}_3$. The molecules undergo a hindered rotation around their symmetry axis with an activation energy of about 100 meV (9.6 kJ mol^{-1}) and an infinite temperature correlation time, τ_c^0 , of $3.7 \times 10^{-13} \text{ s}$. Above 180 K, there is experimental evidence of a melting transition of ammonia in $\text{CsAu}\cdot\text{NH}_3$ as observed in pure NH_3 in the same temperature range.

The ^{133}Cs spectral line shapes are asymmetrically broadened, and the nuclei display a frequency-shift-dependent spin–lattice relaxation rate. Both properties were not found in pure CsAu and can be explained consistently within a model of local inhomogeneities induced by a bipolaronic charge transfer to the ammonia background or perhaps a charge density wave. Further investigations are required to validate this conjecture.

Acknowledgment. We gratefully acknowledge financial support by the Fonds der Chemischen Industrie. S.K. thanks G. Denninger for providing the evolutionary algorithm.

References and Notes

- (1) Desclaux, J. P.; Pyykkö, P. *Chem. Phys. Lett.* **1976**, *39*, 300.
- (2) Pyykkö, P.; Desclaux, J. P. *Acc. Chem. Res.* **1979**, *12*, 276.
- (3) Schwerdtfeger, P.; Dolg, M.; Schwarz, W. H.; Bowmaker, G. A.; Boyd, P. D. W. *J. Chem. Phys.* **1989**, *91*, 1762.
- (4) Dupree, R.; Freyland, W.; Warren, W. W., Jr. *Phys. Rev. Lett.* **1980**, *45*, 130.
- (5) Spicer, W. E.; Sommer, A. H.; White, J. E. *Phys. Rev.* **1959**, *115*, 57.
- (6) Dupree, R.; Kirby, D. J.; Warren, W. W., Jr. *Phys. Rev. B* **1985**, *31*, 5597.
- (7) Mudring, A.-V.; Jansen, M.; Daniels, J.; Krämer, S.; Mehring, M.; Ramalho, J. P.; Romero, A. H.; Parrinello, M. *Angew. Chem.* **2002**, *114*, 128.
- (8) Mudring, A.-V. *Ein Beitrag zur Chemie des Goldes – Darstellung, Struktur und Eigenschaften von Auriden, Auraten und Auridauraten*; Wissenschaft und Technik Verlag: Berlin, 2001.
- (9) Feldmann, C.; Jansen, M. *J. Chem. Soc., Chem. Commun.* **1994**, 1045.
- (10) Acrivos, J. V.; Mott, N. F.; Yoffe, A. D., Eds. *Physics and Chemistry of Electrons and Ions in Condensed Matter*; D. Reidel: Dordrecht, Netherlands, 1984.
- (11) Deng, Z.; Martyna, G. J.; Klein, M. L. *Phys. Rev. Lett.* **1992**, *68*, 2496.
- (12) Wagner, F. E.; Mudring, A.-V.; Jansen, M., manuscript in preparation.
- (13) Tinelli, G. A.; Holcomb, D. F. *J. Solid State Chem.* **1978**, *25*, 157.
- (14) Carolan, J. L.; Scott, T. A. *J. Magn. Reson.* **1970**, *2*, 243.
- (15) Hughes, T. R., Jr. *J. Chem. Phys.* **1963**, *38*, 202.
- (16) Edwards, P. P. In *Physics and Chemistry of Electrons and Ions in Condensed Matter*; Acrivos, J. V., Mott, N. F., Yoffe, A. D., Eds.; D. Reidel: Dordrecht, Netherlands 1984; p 297.
- (17) Butz, T. *Nuclear Spectroscopy on Charge Density Wave Systems*; Kluwer: Dordrecht, Netherlands, 1992.
- (18) Hackspill, L. *Helv. Chim. Acta* **1928**, *11*, 1008.
- (19) Vanino, L. *Handbuch der Präparativen Anorganischen Chemie*; Enke: Stuttgart, Germany, 1921; Vol. 1.
- (20) Baud, M. F.; Hubbard, P. S. *Phys. Rev.* **1968**, *170*, 384.
- (21) Mehring, M.; Raber, H. *J. Chem. Phys.* **1973**, *59*, 1116.
- (22) Runnels, L. K. *Phys. Rev.* **1964**, *134*, A28.
- (23) Hilt, R. A.; Hubbard, P. S. *Phys. Rev.* **1964**, *134*, A392.
- (24) Kubo, R.; Tomita, K. *J. Phys. Soc. Jpn.* **1954**, *9*, 888.
- (25) Bloembergen, N.; Purcell, E. M.; Pound, R. V. *Phys. Rev.* **1948**, *73*, 679.
- (26) Abragam, A. *Principles of Nuclear Magnetism*; Oxford University Press: Oxford, U.K., 1989.
- (27) Mehring, M. *Principles of High-Resolution NMR in Solids*; Springer, Berlin, 1983; Chapter 8.
- (28) Cohen, M. H.; Reif, F. *Solid State Phys.* **1957**, *5*, 321.
- (29) Freude, D.; Haase, J. *NMR Basic Principles and Progress*; Springer: Berlin, 1993; Vol. 29, p 1.
- (30) Mehring, M.; Kanert, O. *Z. Naturforsch.* **1969**, *24a*, 768.
- (31) Lindman, B.; Forsen, S. In *NMR and the Periodic Table*; Harris, R. K., Mann, B. E., Eds.; Academic Press: London, 1978; Chapter 6, p 129.
- (32) Duncan, T. M. *A Compilation of Chemical Shift Anisotropies*; Farragut Press: Chicago, IL, 1990.
- (33) Anderson, P. W. *Phys. Rev.* **1958**, *109*, 1492.
- (34) Mott, N. F.; Kaveh, M. *Adv. Phys.* **1985**, *34* (3), 329.